# Modulation of Bax and mTOR for cancer therapeutics

Rui Li[1, 6], Chunyong Ding[4, 6], Jun Zhang [2, 6, 7], Maohua Xie[1] , Dongkyoo Park[1], Ye Ding[4], Guo Chen[1], Guojing Zhang[2], Melissa Gilbert-Ross[2], Wei Zhou[2], Adam I. Marcus[2], Shi-Yong Sun[2], Zhuo G. Chen[2], Gabriel L. Sica[3], Suresh S. Ramalingam[2], Andrew T. Magis[5], Haian Fu[2], Fadlo R. Khuri[2], Walter J. Curran[1], Taofeek K. Owonikoko[2], Dong M. Shin[2*], Jia Zhou[4*], and Xingming Deng[1*]

Departments of [1]Radiation Oncology, [2]Hematology and Medical Oncology and [3]Pathology, Emory University School of Medicine and Winship Cancer Institute of Emory University, Atlanta, GA 30322; [4]Chemical Biology Program, Department of Pharmacology and Toxicology, University of Texas Medical Branch, Galveston, TX 77555; [5]Institute for Systems Biology, Seattle, WA 98109, USA

[6]Co-first author

[7]Present Address: Department of Internal Medicine, Division of Hematology, Oncology and Blood & Marrow Transplantation, Holden Comprehensive Cancer Center, University of Iowa Carver College of Medicine, 200 Hawkins Drive, Iowa City, IA 52242

**Running Title**: Bax agonist synergizes with RAD001 against cancer

**Disclosure of Potential Conflicts of Interest**
The authors disclose no potential conflicts of interest

[*]**Corresponding Author**: Xingming Deng, Division of Cancer Biology, Department of Radiation Oncology, Emory University School of Medicine, Winship Cancer Institute of Emory University, Atlanta, GA 30322, USA. Phone: (404)778-3398, E-mail: xdeng4@emory.edu, Fax: (404)778-1909; Jia Zhou, Chemical Biology Program, Department of Pharmacology and Toxicology, University of Texas Medical Branch, Galveston, TX 77555. Phone: (409) 772-9748, E-mail: jizhou@utmb.edu, Fax: (409) 772-9648; Dong M. Shin, Department of Hematology and Medical Oncology, Emory University School of Medicine, Winship Cancer Institute of Emory University, Atlanta, Ga 30322, USA. Phone:(404)778-5990. Email: dmshin@emory.edu, Fax:404-778-5220.

This work was supported by National Institutes of Health grants 2R01CA136534-06 (X. Deng), R01CA193828 (X. Deng), 1R01CA200905-01A1 (X. Deng), R01CA140571 (W. Zhou), P50 CA097007 (J. Zhou), P30 DA028821 (J. Zhou) and T32CA160040 (D.M. Shin) as well as R. A. Welch Foundation Chemistry and Biology Collaborative Grant from Gulf Coast Consortia (GCC) for Chemical Genomics, Cancer Prevention and Research Institute of Texas (CPRIT) awards (J. Zhou), and John Sealy Memorial Endowment Fund (J. Zhou). Research reported in this publication was also supported in part by by the Winship Research Pathology and Intergrated Cellular Imaging shared resource, the cores supported by the Winship Cancer Institute of Emory University (P30CAJ 38292), and by the Winship Fashion a Cure Research Scholar Award (X. Deng), a philanthropic award provided by the Winship Cancer Institute of Emory University.

## Abstract

**A rationale exists for pharmacologic manipulation of the serine (S)184 phosphorylation site of the proapoptotic Bcl2 family member Bax as an anticancer strategy. Here we report the refinement of the Bax agonist SMBA1 to generate CYD-2-11, which has characteristics of a suitable clinical lead compound. CYD-2-11 targeted the structural pocket proximal to S184 in the C-terminal region of Bax, directly activating its proapoptotic activity by inducing a conformational change enabling formation of Bax homooligomers in mitochondrial membranes. In murine models of small cell and non-small cell lung cancers, including patient-derived xenograft and the genetically engineered mutant KRAS-driven lung cancer models, CYD-2-11 suppressed malignant growth without evident significant toxicity to normal tissues. In lung cancer patients treated with mTOR inhibitor RAD001, we observed enhanced S184 Bax phosphorylation in lung cancer cells and tissues which inactivates the propaoptotic function of Bax, contributing to rapalog resistance. Combined treatment of CYD-2-11 and RAD001 in murine lung cancer models displayed strong synergistic activity and overcame rapalog resistance in vitro and in vivo. Taken together, our findings provide preclinical evidence for a pharmacologic combination of Bax activation and mTOR inhibition as a rational strategy to improve lung cancer treatment.**

## Introduction

Lung cancer has poor prognosis in part because of innate and acquired resistance to conventional therapies. In order to improve the survival of lung cancer patients, basic molecular mechanisms responsible for resistance to therapy must be carefully elucidated and such knowledge exploited for the development of more effective therapeutic agents. Bax functions as an essential gateway to apoptotic cell death (1) and therefore represents an attractive target for anticancer therapy. We and others recently discovered that AKT-mediated phosphorylation of Bax at serine (S)184 results in the failure of Bax to target or insert into mitochondrial membranes, leading to loss of its cell killing activity (2-4). Conversely, dephosphorylation of Bax at S184 causes a conformational change that promotes the insertion of Bax into mitochondrial membranes and formation of Bax oligomers leading to cytochrome c release and apoptosis (5). Thus, the S184 phosphorylation site is a critical switch to functionally control the proapoptotic activity of Bax (3, 5). Notably, the structural pocket around the S184 residue in the Bax protein represents an ideal target for small molecule docking (6, 7). This binding pocket is located in the hydrophobic C-terminal tail of Bax, which regulates not only the subcellular location of Bax but also its ability to insert into mitochondrial membranes (3, 5, 8).

Although mTOR is a promising therapeutic target in lung cancer (9-11), mTOR inhibition by rapalogs has been reported to block an S6K1-IRS1 negative feedback loop leading to the activation of PI3K/AKT proliferative and prosurvival signals, and thus countering the anticancer efficacy of rapalogs (12, 13). AKT is a known upstream Bax kinase that can directly phosphorylate Bax at the S184 site leading to Bax inactivation (4). Here we discovered that the rapalog-induced activation of AKT enhances Bax phosphorylation and inactivates the

proapoptotic function of Bax. Using an *in silico* screening approach, we have recently identified three small molecule Bax agonists (SMBA1-3) that specifically bind the structural pocket around the S184 residue of Bax protein leading to activation of the proapoptotic function of Bax (7). Based on chemical structure and drug-likeness, we chose SMBA1 as the lead compound and generated a more effective analog CYD-2-11, which not only reverses rapalog-resistance but also synergizes with the mTOR inhibitor RAD001 against lung cancer.

## Materials and Methods

### Materials

SMBA1 and CYD-2-11 compounds were chemically synthesized by Dr. Zhou's laboratory, University of Texas Medical Branch. RAD001 and BEZ235 were purchased from Selleck Chemicals (Houston, TX). Anti-Bax (catalog # sc-493) and β-actin were purchased from Santa Cruz Biotechnology (Santa Cruz, CA). Bax 6A7 and Cyt c antibodies were obtained from BD PharMingen (San Diego, CA). Phospho-specific S184 Bax (pBax) antibody was purchased from Abcam (Cambridge, MA). Antibodies against active caspase 3, Akt, mTOR, pAKT (S473) and p-p70S6K were purchased from Cell Signaling Technology (Beverly, MA). Fluorescent Bak peptide (FAM-GQVGRQLAIIGDDINR) and Bcl-XL protein were purchased from NeoBioSci™ (Cambridge, MA). Purified recombinant full-length human Bcl2 protein was obtained from Protein*X* Lab (San Diego, CA). Purified full-length human Mcl-1 protein was purchased from GenWay Biotech, Inc. (San Diego, CA). Purified full-length human Bfl-1/A1 protein was obtained from R&D systems (Minneapolis, MN). Purified full-length human Bax protein was purchased from Novus (Littleton, CO). Bis(maleimido) hexane (BMH) was purchased from Thermo Scientific. QD605 goat anti-rabbit IgG conjugate (red), QD705 goat

anti-mouse IgG conjugate (green) and ProLong® Gold antifade reagent with 4', 6-diamidino-2-phenylindole (DAPI) were obtained from Invitrogen Life Technologies Inc (Carlsbad, CA). Cre-adenovirus (Ad5CMVCre; Cat #: VVC-U of Iowa-5) was obtained from Viral Vector Core Facility of the University of Iowa. All reagents used were obtained from commercial sources unless otherwise stated.

**Cell lines and cell culture**

NSCLC, SCLC and normal human bronchial epithelial (BEAS-2B) cell lines were obtained from the American Type Culture Collection (Manassas, VA). Human NSCLC cell lines (H1299, H292, H157, Calu-1, H460 and H1975) were maintained in RPMI 1640 with 10% fetal bovine serum (FBS). A549 cells were cultured in F-12K medium with 10% FBS. BEAS-2B cells were cultured in DMEM/F-12 medium with 10% FBS. SCLC cell lines DMS53, DMS153, DMS114, H128, H146 and H69 were cultured in Weymouth's medium with 5% FBS and 5% bovine serum (BS) as described (14). The rapamycin resistant A549 cell line (A549-RR) was established as described (10, 15), and is also resistant to rapalog RAD001. These cell lines were employed for the described experiments without further authentication by authors.

**Human clinical trial patient samples and establishment of patient-derived xenografts (PDX)**

Informed consent was obtained from all human subjects, and use of human samples for immunohistochemistry and PDX was approved by the Institutional Review Board (IRB) of Emory University. Paired samples of NSCLC tissues were collected as part of a completed phase I clinical trial evaluating the pharmacodynamic effects of RAD001 in adult patients with resectable NSCLC. Enrolled eligible patients received RAD001 (10 mg) orally once daily for 28 days (16). Pretreatment biopsy samples and post treatment surgical resection specimens were

analyzed for pBax (S184) expression. PDXs (TKO-002 and TKO-005) were obtained as part of an IRB-approved phase II co-clinical trial of arsenic trioxide in patients with relapsed SCLC who had failed standard platinum-based chemotherapy. Tumor samples were obtained by image-guided biopsy and were directly implanted into Nu/Nu nude mice without intervening propagation in plastic culture plates. Direct serial propagation of growing tumor occurred for up to 5 generations. The animal propagation protocol was approved by the Emory IACUC and the Emory Animal Ethics Committee.

**Genetically engineered mouse model (GEMM), treatment and tumor burden quantification**

Mouse strains harboring a conditional activating mutation (G12D) at the endogenous KRAS locus and conditional LKB1 knockout were previously described (17). Lox-stop-lox (LSL)-$KRAS^{G12D}$ $LKB1^{fl/fl}$ (*i.e*. KL) mice were generated by intercrossing the B6.129S4-Krastm3Tyj/J ($K\text{-}Ras^{G12D}$) and FVB; 129S6-Stk11tm1Rdp/Nci (LKB1) strains for two generations and genotyped to confirm homozygosity for the LKB1 allele as described (17-20). All studies were performed on protocols approved by the Emory University IACUC. Six weeks after intranasal administration of $5x10^6$ pfu AdeCre, mice were treated with CYD-2-11 i.p for 8 weeks. Mice were sacrificed by inhaled $CO_2$ at the end of treatment. After lung perfusion with PBS, the left lung lobes were harvested from mice in control and CYD-2-11 treated groups and immediately fixed in 10% neutral buffered formalin (Fisher Scientific, Kalamazoo, MI), horizontally cut into three equal parts and embedded in paraffin blocks. Three parts of lung tissues representing different regions of the lung were vertically put into paraffin blocks for hematoxin-eosin (H&E) staining. Lung tissue samples were sectioned at 3 μm three times for placement of slides and stained with H&E. H&E stained samples were scanned using Nano Zoomer 2.0-HT

(Hamamatsu, Japan) and images were analyzed using ImageScope viewing software (Leica Biosystems, Buffalo Grove, IL). Tumor numbers were counted under a microscope and tumor area was quantified using Openlab modular imaging software (PerkinElmer, Waltham, MA).

### Statistical analysis

The statistical significance of differences between two groups was analyzed with two-sided unpaired student's t-test. Results were considered to be statistically significant at $p < 0.05$. Statistical analysis was performed with Graphpad InStat 3 software (San Diego, CA) (21).

## Results

### Generation of new SMBA analog CYD-2-11

We have recently identified three small molecule Bax agonist compounds (SMBA1, SMBA2 and SMBA3) (7). Based on comparison analyses of S184 docking and the chemical structures as well as drug-likeness, we selected SMBA1 as the best lead compound of the three molecules for further SAR studies. Our molecular docking analysis revealed that introduction of an *O*-alkylamino side chain tethered to the hydroxyl group on the phenyl ring of lead compound SMBA1 (**Figure 1A and B**) could enhance the pharmacophore group to access a deeper binding pocket near S184 and improve Bax binding. The resulting analog CYD-2-11 docks well into the binding pocket of Bax (**Figure 1C)**, and the *O*-alkylamino side chain can form hydrogen-bonds with the amino acid residues around the S184 site (**Figure 1C**). Moreover, the terminal amino group of CYD-2-11 can form an HCl salt to improve aqueous solubility and lead to a favorable LogP value of the molecule for better cell permeability. SMBA1 was synthesized by coupling of the commercially available material 2-nitro-9*H*-fluorene with salicylaldehyde in the presence of KF-$Al_2O_3$ as a solid base in methanol with 72% yield.

Analogue CYD-2-11 was synthesized using the Mitsunobu reaction from phenol SMBA1 with Boc-protected aminoethanol, followed by subsequent Boc-deprotection in a two-step process, with a yield of 73%.

**CYD-2-11 specifically binds to Bax protein and induces apoptosis of human lung cancer cells**

Computational modeling analysis reveals that CYD-2-11 docks at the S184 binding pocket of Bax (**Figure 1C**). Bax and Bak proteins can heterodimerize via their BH3 domains to form Bax/Bak heterodimers (22). A fluorescently-labeled Bak BH3 domain peptide binds to the Bax protein with high-affinity (7). This Bak BH3 domain peptide is located in Bak BH3 domain as shown in **Figure S1**. We used this peptide to quantify CYD-2-11/Bax binding affinity in a competition fluorescence polarization assay as described (23-25). Results indicate that CYD-2-11 directly binds to Bax protein with high affinity ($K_i$: 34.1 ± 8.54 nM) (**Figure 1D**). CYD-2-11 failed to bind other Bcl2 family members (*i.e*. Bak, Bid, Bcl2, Bcl-XL, Bcl-w, Mcl-1 and A1) *in vitro* (**Figure 1D**), indicating a binding selectivity for Bax protein. The apoptotic effect of CYD-2-11 was measured in both SCLC and NSCLC cell lines that express various levels of endogenous pBax/Bax by analysis of Annexin-V/PI binding by fluorescence-activated cell sorter (FACS) as we previously described (26, 27). It appears that human lung cancer cells expressing higher levels of total Bax also contain relatively higher levels of pBax (**Figure 1E**). CYD-2-11 was more potent than SMBA1 in inducing apoptosis in both NSCLC and SCLC cell lines. NSCLC cell lines (*i.e.* H292, H157, H1975, A549) and SCLC cell lines (*i.e*. DMS53 and DMS153) that express relatively high levels of pBax/Bax were more sensitive to induction of apoptosis by CYD-2-11. In contrast, lung cancer cell lines expressing relatively low levels of

pBax/Bax (*i.e*. NSCLC cell line: H460; SCLC cell lines: DMS114 and H128) were relatively less sensitive to CYD-2-11 (**Figure 1E and F**). To confirm the anti-phospho Bax (S184) antibody is totally selective to the phosphorylated form of Bax, we used protein phosphatase (λPPase) to treat immunoprecipitated Bax from A549 cells. pBax was analyzed by anti-phospho-specific Bax antibody. Results reveal that λPPase removed phosphate from S184 phosphorylated Bax but has no effect on total Bax level (**Figure S2**), suggesting that the anti-phospho Bax (S184) antibody we used is totally selective to the pBax. Based on our findings, we propose that the cytotoxicity of CYD-2-11 may be dependent on the expression levels of pBax and/or total Bax in lung cancer cell lines. Importantly, CYD-2-11 showed less cytotoxicity in the normal lung epithelial cell line (BEAS-2B), which expresses a low level of endogenous pBax (**Figure 1E and F**), indicating a relative selectivity against cancer cells compared to normal cells. These findings suggest that CYD-2-11 may have strong potential to be developed as a new class of anti-cancer agents.

**CYD-2-11 directly activates the proapoptotic function of Bax via oligomerization leading to cytochrome c (Cyt c) release from mitochondria**

Our results indicate that treatment of human lung cancer A549 cells with CYD-2-11 did not affect Bax protein level (**Figure 2A**). It is known that Bax oligomerization can activate the proapoptotic function of Bax because Bax oligomers can form a pore with a size that is capable of transporting Cyt c (28). To assess whether CYD-2-11 regulates the ability of membrane-inserted Bax to form oligomers in the mitochondrial membrane, a cross-linking study with Bis (maleimido) hexane (BMH) was performed to measure Bax oligomerization as we previously as described (7, 22, 29). Intriguingly, direct treatment of mitochondria isolated from A549 cells with CYD-2-11 (5 μM) facilitated the formation of Bax dimers and trimers

(**Figure 2B**, left panel). SMBA1 was used as a positive control (7). The molecular sizes of these adducts were estimated to be multiples of ~21 kDa, suggesting the formation of Bax homo-oligomers in isolated mitochondria. To further test whether CYD-2-11 activates Bax through the formation of oligomers in A549 cells, cross linking studies with BHM were employed following treatment of A549 cells with CYD-2-11 as described (7, 22, 29). Results indicate that treatment of A549 cells with CYD-2-11 or SMBA1 resulted in the formation of Bax dimers and trimers in A549 cells (**Figure 2B**, right panel). The pattern of Bax oligomers was similar to that in the treated mitochondria above. Since CYD-2-11 failed to induce BAK oligomerization in isolated mitochondria (**Figure S3**), this indiccates that such effect of CYD-2-11 is specific for Bax. These findings provide evidence that CYD-2-11 can directly activate Bax but not BAK through its oligomerization in isolated mitochondrial membranes.

Sucellular fractionation experiments further demonstrated that treatment of A549 cells with CYD-2-11 led to Cyt c release from mitochondria into cytosol in association with Bax accumulation in mitochondria (**Figure 2C**).

**CYD-2-11 suppresses lung cancer growth via induction of apoptosis in NSCLC and SCLC xenografts as well as PDX models**

To test the *in vivo* efficacy of CYD-2-11, we used nude mice and the human lung cancer A549 cell line to produce subcutaneous (s.c.) lung tumor xenografts as described (30, 31). Mice were treated with increasing doses of CYD-2-11 intraperitoneally (i.p.) for 10 days. CYD-2-11 induced a dose-dependent repression of lung cancer growth *in vivo* (**Figure 2D**). To test whether CYD-2-11 suppression of lung cancer occurs through activation of Bax leading to apoptosis in lung tumor tissues, active caspase 3 and Bax oligomerization in tumor tissues were measured by IHC or cross-linking, respectively. Treatment of lung cancer xenograft mice

with CYD-2-11 resulted in Bax oligomerization and caspase 3 activation (**Figure 2E, F and G**). No weight loss, no significant increase in ALT, AST and BUN or decrease in WBC, RBC, Hb and PLT were observed following CYD-2-11 treatment (**Figure S4**). Histopathologic evaluation of harvested normal tissues (brain, heart, lung, liver, spleen, kidney and intestine) revealed no evidence of normal tissue toxicity (**Figure S4**).

To compare the *in vivo* efficacy of CYD-2-11 with that of SMBA1, NSCLC (A549) and SCLC (DMS53) xenografts were treated with 40mg/kg of CYD-2-11 or SMBA1 i.p. for 14 days. CYD-2-11 exhibited more potent anti-tumor activity than SMBA1 in both NSCLC and SCLC xenografts (**Figure 3**).

To evaluate the anti-tumor activity of CYD-2-11 in patient-derived xenografts (PDX), we employed two PDXs (TKO-002 and TKO-005) derived from tumor tissue biopsies from patients with relapsed SCLC. Given that these two PDXs were derived from patients without intervening *in vitro* culture, they are expected to closely recapitulate the SCLC tumor setting. Mice with TKO-002 and TKO-005 PDXs were treated with CYD-2-11 (40mg/kg/d) i.p. for 2 weeks. CYD-2-11 potently suppressed the growth of both SCLC TKO-002 and TKO-005 PDXs (**Figure 4A**). To examine whether CYD-2-11 can convert Bax from its inactive (pS184 Bax) to active (6A7 Bax) form in PDX tumor tissues, quantum dot-based immunohistofluorescence (QD-IHF) was performed as we previously described (7, 32). pBax and 6A7 Bax were analyzed simultaneously by QD-IHF on the same tissue slide using primary antibodies from different sources (rabbit anti-pBax and mouse anti-6A7) and QD-conjugated anti-rabbit [QD605 (red)] and anti-mouse [QD705 (green)] secondary antibodies with two different emission wavelengths. Separated and combined QD images were obtained after determining the QD spectral library and unmixing the cubed image. Treatment of SCLC PDX mice with

CYD-2-11 (40mg/kg/d) resulted in downregulation of phosphorylated Bax (pBax) and upregulation of conformationally changed Bax (6A7 Bax) in tumor tissues (**Figure 4B**). Total Bax levels had no significant change (**Figure S5**). These findings suggest that CYD-2-11 is able to convert Bax from the inactive (pBax) to activated (6A7 Bax) form, eventually leading to apoptosis in tumor tissues. Furthermore, Bax oligomerization and apoptosis (*i.e*. active caspase 3) were also observed in tumor tissues (**Figure 4CD**). No significant normal tissue toxicity was observed (**Figure S6**). These findings indicate that CYD-2-11 may potentially be effective in patients with SCLC, for which there are currently limited treatment options.

**CYD-2-11 displays potent anti-tumor activity against KRAS-driven lung cancer in genetically engineered mouse models (GEMM)**

KRAS is the most commonly mutated oncogene, yet no effective targeted therapies exist for KRAS-mutant cancers (33). Here we found that expression of exogenous constitutively active KRAS (G12D) mutant in H1944 cells with wild-type KRAS background significantly enhanced Bax phosphorylation at S184 in association with activation of upstream Bax kinase AKT (**Figure S7A**). Since CYD-2-11 can convert Bax from its inactive form (*i.e*. pBax) to the activated form (*i.e*. 6A7 Bax) to induce apoptosis (**Figure 4B**), this indicates that CYD-2-11 may be effective for the treatment of KRAS mutant-driven cancer. To test the potency of CYD-2-11 in KRAS mutant-driven lung cancer, lox-stop-lox (LSL)-$KRAS^{G12D}$ $LKB1^{fl/fl}$ (*i.e*. KL) mice were generated and bred out as previously described (17-20). These mice contain a $KRAS^{G12D}$ LSL knock-in allele and a floxed allele of LKB1 ($LKB1^{fl/fl}$) (17, 18). Primary lung adenocarcinoma was detectable as early as 6 weeks after intranasal administration of $5x10^6$ pfu adenovirus expressing Cre recombinase (AdeCre) in $KRAS^{G12D}$ $LKB1^{fl/fl}$ (KL) mice (**Figure**

**S7BC**). It has been previously reported that pAKT is upregulated in lung tumor tissues from KL mice (34). Since AKT is a physiological Bax kinase (3, 4), activated AKT may phosphorylate Bax in KL mice. As expected, increased Bax phosphorylation (S184) was observed in tumor tissues from KL mice as compared to adjacent normal lung tissues (**Figure S7D**), thereby providing a good rationale to employ Bax agonist (CYD-2-11) for the treatment of KRAS-driven lung cancer. In order to further assess the potential of CYD-2-11 as therapy for KRAS-driven lung cancer, CYD-2-11 (40mg/kg/d) or vehicle was administered i.p. starting at 6 weeks post AdeCre delivery as previously suggested (18). After treatment for 8 weeks, mice were euthanized with $CO_2$ asphyxiation. Lungs with tumor and normal lung tissues were collected for further analysis. To quantify tumor burden and tumor multiplicity in mice, H&E-stained lungs were imaged with morphometric software to quantify the surface area composed of tumor as opposed to normal tissue of representative cross-sections of each lung lobe for each mouse as shown in **Figure S8** and previously described (18). Results indicate that treatment of KL mice with CYD-2-11 for 8 weeks resulted in significant reduction of tumor burden and multiplicity in the lung via apoptosis (**Figure 5A, B and C**). Importantly, treatment with CYD-2-11 significantly prolonged survival of KL mice when compared with the control group (**Figure 5D**). There were 5 deaths out of 8 mice in the control group versus 2 deaths out of 7 mice in the CYD-2-11 treatment group ($p < 0.01$), calculated up to 8 weeks before euthanization. No normal tissue toxicity was observed during treatment (**Figure S9**).

**mTOR inhibition by RAD001 enhances Bax phosphorylation in lung cancer cells and tumor tissues from NSCLC patients**

Rapamycin and its derivative RAD001 (*i.e*. everolimus) are potent allosteric inhibitors of mTOR (35). RAD001 is well tolerated but shows limited antitumor activity as a single agent in patients

with lung cancer (36-38). Previous reports indicate that inhibition of mTOR by rapamycin or RAD001 results in activation of AKT (12, 13), which is an upstream Bax kinase (3, 4). To further test whether mTOR inhibition actually promotes Bax phosphorylation in human lung cancer cells, A549 cells were treated with increasing concentrations of RAD001 for 24hr. Western blot and QD-IHF studies indicate that inhibition of mTOR by RAD001 resulted in activation of AKT and upregulation of S184 Bax phosphorylation (**Figure 6A and B**). To test whether a similar effect of RAD001 on Bax phosphorylation occurs in patient tumors, we analyzed pBax by IHC in baseline and post-treatment tissue samples obtained from 10 NSCLC patients treated with RAD001 (10 mg/day) for 28 days as part of a neoadjuvant phase Ib clinical study of everolimus in patients with resectable NSCLC (16). There was increased Bax phosphorylation in post-treatment tumor tissues compared to baseline samples (**Figure 6C and D**). These findings suggest that mTOR inhibition-induced Bax phosphorylation and inactivation of the proapoptotic function of Bax may negatively affect the sensitivity of lung cancer to mTOR inhibitor. This suggests that, as a Bax agonist, CYD-2-11 may have strong potential to enhance the potency of mTOR inhibitor against lung cancer.

BEZ235 is a dual PI3K/mTOR inhibitor (39). We also tested the effect of BEZ235 on AKT activity and Bax phosphorylation. As expected, BEZ235 not only inhibited mTOR activity (*i.e*. reduced p-p70S6K) but also suppressed AKT activity in A549 cells. Intriguingly, treatment of A549 cells with BEZ235 did not enhance Bax phosphorylation, inversely, reduced Bax phosphorylation (**Figure S10**). This may occur through inhibition of AKT (*i.e*. Bax kinase) activity, further demonstrated that AKT is critical for Bax phosphorylation.

**CYD-2-11 and RAD001 synergistically repress lung cancer growth and overcome rapalog resistance *in vitro* and *in vivo***

To determine whether Bax phosphorylation contributes to acquired resistance to RAD001, we established a RAD001-resistant strain from the parental A549 cell line (*i.e*. A549-RR) as we previously described (15). Increased levels of pBax were observed in A549-RR cells as compared to parental A549 cells (**Figure S11A and B**). As expected, parental A549 cells remained sensitive while A549-RR cells were resistant to RAD001 (**Figure S11C and D**). These results provide strong evidence that RAD001-enhanced Bax phosphorylation contributes to acquired RAD001 resistance. Intriguingly, A549-RR cells were resistant to RAD001 but remained sensitive to CYD-2-11 (**Figure S11C and D**), suggesting that CYD-2-11 can reverse acquired RAD001 resistance through conversion of Bax from the inactive to active form. To test whether CYD-2-11 overcomes RAD001 resistance *in vivo*, NSCLC xenografts derived from A549 and A549-RR cell lines were treated with continuous daily dosing of RAD001 (1 mg/kg) and CYD-2-11 (40 mg/kg) alone or in combination for 2 weeks. We observed that lung cancer xenografts derived from A549 parental cells were sensitive whereas xenografts derived from A549-RR cells were resistant to RAD001 (**Figure 7A, left vs. right panel**). Consistent with the *in vitro* observations, CYD-2-11 and RAD001 synergistically repressed both A549 and A549-RR xenografts (**Figure 7A**), indicating that CYD-2-11 can overcome acquired RAD001 resistance *in vivo*. QD-IHF studies revealed that CYD-2-11 blocked RAD001-stimulated Bax phosphorylation and coverted Bax from the inactive (pBax) to active form (6A7 Bax) in tumor tissues (**Figure 7B**), which promoted caspase activation and apoptosis (**Figure 7C and D**). Total Bax levels had no significant change (**Figure S12**).There were no significant normal tissue toxicities (**Figure S13**). Furthermore, CYD-2-11 in combination with RAD001 exhibited significantly more potent antitumor activity than either CYD-2-11 or RAD001 alone in a SCLC PDX model (**Figure S14**).

## Discussion

Induction of apoptosis is a critical mechanism underlying the durable efficacy of cancer treatment agents. Bax is a major proapoptotic protein whose activation is required for cell death (1). Understanding the cellular mechanisms required for Bax activation is of great significance because of the potential to exploit this knowledge to develop new approaches and agents for cancer therapy. We have recently identified three small molecule Bax agonists, including SMBA1, SMBA2 and SMBA3, that target the structural pocket around S184 in the C-terminal tail of Bax and activate the propapoptotic function of Bax (7). Based on its chemical structure and drug-likeness, we chose SMBA1 as the lead and generated an SMBA1 analog CYD-2-11 that has improved potency against lung cancer. CYD-2-11 selectively binds to Bax in the pocket around the S184 phosphorylation site, with no binding to other Bcl2 family members, and induces apoptosis of various lung cancer cell lines more potently than SMBA1 (**Figure 1**). Mechanistically, CYD-2-11 directly induces Bax oligomerization in isolated mitochondria and lung cancer A549 cells (**Figure 2B**) as well as in tumor tissues from A549 xenografts or PDXs (**Figures 2-4**), indicating a direct mechanism by which CYD-2-11 activates Bax protein. It is known that oligomerization of Bax molecules in mitochondria is a major mechanism through which Bax induces cytochrome c (Cyt c) release (28). These findings help explain how CYD-2-11 triggers Cyt c release in lung cancer A549 cells (**Figure 2C**). Intriguingly, CYD-2-11 suppresses A549 xenograft tumor growth via Bax activation and induction of apoptosis in tumor tissues in a dose-dependent manner (**Figure 2D-G**). CYD-2-11 displays more potent antitumor activity than SMBA1 against both NSCLC and SCLC xenografts (**Figure 3**). QD-based images showed that CYD-2-11 can reduce levels of the inactive form of Bax (pS184 Bax) and enhance the activated form of Bax (*i.e.*, 6A7

conformationally changed Bax) in tumor tissues from PDXs and A549 xenografts (**Figures 4 and 7**). Based on these findings, we propose that CYD-2-11-induced suppression of lung cancer may result from selective activation of the proapoptotic function of Bax leading to increased apoptosis in tumors.

PDX models have been considered as more advanced preclinical cancer models, which mostly retain the principal histologic and genetic characteristics of their donor tumors and remain stable across passages. Combined clinical and PDX studies have shown a high degree of correlation between clinical response to cytotoxic agents in adult patients with lung cancer and response to the same agents in PDX models generated from these patients (40). PDX models have been shown to be predictive of clinical outcomes and are being used for preclinical and clinical drug evaluation (41, 42). Since CYD-2-11 effectively suppressed the growth of two PDXs (TKO-002 and TKO-005) raised from two patients with refractory SCLC (**Figure 4**), there is good potential for CYD-2-11 to provide clinical potency in patients with chemorefractory SCLC in the future.

In addition to PDX models, genetically engineered mouse models (GEMM) are also considered to be advanced preclinical cancer models. It is known that genetically engineered mice (GEM) are the most sophisticated animal models of human cancer, which closely recapitulate the pathophysiological process of human malignancies in genetically precisely defined systems (43). Therefore, the potency of CYD-2-11 was also evaluated in genetically engineered KL mice. Since pS184 Bax (inactive form) is significantly upregulated in tumor tissues from KL mice (**Figure S7**), CYD-2-11, as a Bax agonist, should be an ideal agent for treatment of KRAS-driven lung cancer. Intriguingly, CYD-2-11 significantly reduces tumor burden in the lungs of KL mice leading to prolonged survival when compared with the untreated control

group (**Figure 5**), suggesting that CYD-2-11 has the potential to improve the prognosis of lung cancer patients with KRAS mutations.

mTOR is a promising therapeutic target in lung cancer (9-11). However, mTOR inhibition by rapalogs has been reported to activate PI3K/AKT proliferative and prosurvival signals thereby attenuating anticancer efficacy (12, 13, 44). Here, we discovered that inhibition of mTOR by RAD001 not only activates AKT but also leads to S184 Bax phosphorylation and inactivation in a lung cancer cell line and in tumor tissues from NSCLC patients treated with RAD001 (**Figure 6**). It is possible that Bax phosphorylation induced by mTOR inhibitor therapy may negatively affect the efficacy of mTOR inhibitor in cancer therapy. This may explain the limited efficacy of single-agent RAD001 in lung cancer patients (36, 37). Furthermore, the phosphorylated form of Bax (pBax) was found to accumulate in RAD001 resistant cells (A549-RR) (**Figure S11AB**), indicating that pBax may contribute to rapalog resistance. Our findings provide a strong rationale for the combination of mTOR inhibitor (RAD001) with Bax agonist (CYD-2-11), which may have superior therapeutic benefits and may reverse rapalog resistance. As expected, CYD-2-11 in combination with RAD001 not only exhibits strong synergistic activity against lung cancer but also overcomes rapalog resistance *in vitro* (**Figure S11C and D**) and *in vivo* (**Figure 7**).

In summary, we have generated a new Bax agonist CYD-2-11 that selectively targets the structural binding pocket around the S184 phosphorylation site in Bax. The binding of CYD-2-11 with Bax results in a 6A7 conformational change and oligomerization of Bax protein leading to activation of its proapoptotic function. The Bax agonist CYD-2-11 exhibits potent efficacy against human lung cancer *in vivo* without normal tissue toxicity. mTOR inhibition by RAD001 leads to S184 Bax phosphorylation contributing to rapalog resistance. Co-targeting mTOR and

Bax via a mechanism-driven combination of mTOR inhibitor and Bax agonist represents a more effective therapeutic approach for overcoming treatment resistance and improving lung cancer outcome.

## ACKNOWLEDGMENTS

We thank Anthea Hammond for editing of the manuscript.

## References

1. Wei MC, Zong WX, Cheng EH, Lindsten T, Panoutsakopoulou V, Ross AJ, et al. Proapoptotic BAX and BAK: a requisite gateway to mitochondrial dysfunction and death. Science. 2001;292:727-30.
2. Wang Q, Sun SY, Khuri F, Curran WJ, Deng X. Mono- or double-site phosphorylation distinctly regulates the proapoptotic function of Bax. PLoS One. 2010;5:e13393.
3. Xin M, Deng X. Nicotine inactivation of the proapoptotic function of Bax through phosphorylation. J Biol Chem. 2005;280:10781-9.
4. Gardai SJ, Hildeman DA, Frankel SK, Whitlock BB, Frasch SC, Borregaard N, et al. Phosphorylation of Bax Ser184 by Akt regulates its activity and apoptosis in neutrophils. J Biol Chem. 2004;279:21085-95.
5. Xin M, Deng X. Protein phosphatase 2A enhances the proapoptotic function of Bax through dephosphorylation. J Biol Chem. 2006;281:18859-67.
6. Suzuki M, Youle RJ, Tjandra N. Structure of Bax: coregulation of dimer formation and intracellular localization. Cell. 2000;103:645-54.
7. Xin M, Li R, Xie M, Park D, Owonikoko TK, Sica GL, et al. Small-molecule Bax agonists for cancer therapy. Nature communications. 2014;5:4935.
8. Nechushtan A, Smith CL, Hsu YT, Youle RJ. Conformation of the Bax C-terminus regulates subcellular location and cell death. EMBO J. 1999;18:2330-41.
9. Johnson BE, Jackman D, Janne PA. Rationale for a phase I trial of erlotinib and the mammalian target of rapamycin inhibitor everolimus (RAD001) for patients with relapsed non small cell lung cancer. Clin Cancer Res. 2007;13:s4628-31.
10. Wang X, Yue P, Kim YA, Fu H, Khuri FR, Sun SY. Enhancing mammalian target of rapamycin (mTOR)-targeted cancer therapy by preventing mTOR/raptor inhibition-initiated, mTOR/rictor-independent Akt activation. Cancer Res. 2008;68:7409-18.
11. Wangpaichitr M, Wu C, You M, Kuo MT, Feun L, Lampidis T, et al. Inhibition of mTOR restores cisplatin sensitivity through down-regulation of growth and anti-apoptotic proteins. Eur J Pharmacol. 2008;591:124-7.

12. O'Reilly KE, Rojo F, She QB, Solit D, Mills GB, Smith D, et al. mTOR inhibition induces upstream receptor tyrosine kinase signaling and activates Akt. Cancer Res. 2006;66:1500-8.
13. Sun SY, Rosenberg LM, Wang X, Zhou Z, Yue P, Fu H, et al. Activation of Akt and eIF4E survival pathways by rapamycin-mediated mammalian target of rapamycin inhibition. Cancer Res. 2005;65:7052-8.
14. Park D, Magis AT, Li R, Owonikoko TK, Sica GL, Sun SY, et al. Novel small-molecule inhibitors of Bcl-XL to treat lung cancer. Cancer Res. 2013;73:5485-96.
15. Liu Y, Sun SY, Owonikoko TK, Sica GL, Curran WJ, Khuri FR, et al. Rapamycin induces Bad phosphorylation in association with its resistance to human lung cancer cells. Mol Cancer Ther. 2012;11:45-56.
16. Owonikoko TK, Ramalingam SS, Miller DL, Force SD, Sica GL, Mendel J, et al. A Translational, Pharmacodynamic, and Pharmacokinetic Phase IB Clinical Study of Everolimus in Resectable Non-Small Cell Lung Cancer. Clin Cancer Res. 2015;21:1859-68.
17. Ji H, Ramsey MR, Hayes DN, Fan C, McNamara K, Kozlowski P, et al. LKB1 modulates lung cancer differentiation and metastasis. Nature. 2007;448:807-10.
18. Shackelford DB, Abt E, Gerken L, Vasquez DS, Seki A, Leblanc M, et al. LKB1 inactivation dictates therapeutic response of non-small cell lung cancer to the metabolism drug phenformin. Cancer Cell. 2013;23:143-58.
19. Jackson EL, Willis N, Mercer K, Bronson RT, Crowley D, Montoya R, et al. Analysis of lung tumor initiation and progression using conditional expression of oncogenic K-ras. Genes Dev. 2001;15:3243-8.
20. Tuveson DA, Shaw AT, Willis NA, Silver DP, Jackson EL, Chang S, et al. Endogenous oncogenic K-ras(G12D) stimulates proliferation and widespread neoplastic and developmental defects. Cancer Cell. 2004;5:375-87.
21. Wang X, Hawk N, Yue P, Kauh J, Ramalingam SS, Fu H, et al. Overcoming mTOR inhibition-induced paradoxical activation of survival signaling pathways enhances mTOR inhibitors' anticancer efficacy. Cancer Biol Ther. 2008;7:1952-8.
22. Dewson G, Ma S, Frederick P, Hockings C, Tan I, Kratina T, et al. Bax dimerizes via a symmetric BH3:groove interface during apoptosis. Cell Death Differ. 2012;19:661-70.
23. Wang JL, Liu D, Zhang ZJ, Shan S, Han X, Srinivasula SM, et al. Structure-based discovery of an organic compound that binds Bcl-2 protein and induces apoptosis of tumor cells. Proc Natl Acad Sci U S A. 2000;97:7124-9.
24. Zhang H, Nimmer P, Rosenberg SH, Ng SC, Joseph M. Development of a high-throughput fluorescence polarization assay for Bcl-x(L). Anal Biochem. 2002;307:70-5.
25. Bruncko M, Oost TK, Belli BA, Ding H, Joseph MK, Kunzer A, et al. Studies leading to potent, dual inhibitors of Bcl-2 and Bcl-xL. J Med Chem. 2007;50:641-62.
26. Deng X, Xiao L, Lang W, Gao F, Ruvolo P, May WS, Jr. Novel role for JNK as a stress-activated Bcl2 kinase. J Biol Chem. 2001;276:23681-8.
27. Deng X, Gao F, Flagg T, Anderson J, May WS. Bcl2's flexible loop domain regulates p53 binding and survival. Mol Cell Biol. 2006;26:4421-34.
28. Saito M, Korsmeyer SJ, Schlesinger PH. BAX-dependent transport of cytochrome c reconstituted in pure liposomes. Nat Cell Biol. 2000;2:553-5.
29. Dewson G, Kratina T, Sim HW, Puthalakath H, Adams JM, Colman PM, et al. To trigger apoptosis, Bak exposes its BH3 domain and homodimerizes via BH3:groove interactions. Mol Cell. 2008;30:369-80.

30. Oltersdorf T, Elmore SW, Shoemaker AR, Armstrong RC, Augeri DJ, Belli BA, et al. An inhibitor of Bcl-2 family proteins induces regression of solid tumours. Nature. 2005;435:677-81.
31. Puri N, Khramtsov A, Ahmed S, Nallasura V, Hetzel JT, Jagadeeswaran R, et al. A selective small molecule inhibitor of c-Met, PHA665752, inhibits tumorigenicity and angiogenesis in mouse lung cancer xenografts. Cancer Res. 2007;67:3529-34.
32. Han B, Park D, Li R, Xie M, Owonikoko TK, Zhang G, et al. Small-Molecule Bcl2 BH4 Antagonist for Lung Cancer Therapy. Cancer Cell. 2015;27:852-63.
33. Corcoran RB, Cheng KA, Hata AN, Faber AC, Ebi H, Coffee EM, et al. Synthetic lethal interaction of combined BCL-XL and MEK inhibition promotes tumor regressions in KRAS mutant cancer models. Cancer cell. 2013;23:121-8.
34. Chen Z, Cheng K, Walton Z, Wang Y, Ebi H, Shimamura T, et al. A murine lung cancer co-clinical trial identifies genetic modifiers of therapeutic response. Nature. 2012;483:613-7.
35. Legrier ME, Yang CP, Yan HG, Lopez-Barcons L, Keller SM, Perez-Soler R, et al. Targeting protein translation in human non small cell lung cancer via combined MEK and mammalian target of rapamycin suppression. Cancer Res. 2007;67:11300-8.
36. Tarhini A, Kotsakis A, Gooding W, Shuai Y, Petro D, Friedland D, et al. Phase II study of everolimus (RAD001) in previously treated small cell lung cancer. Clin Cancer Res. 2010;16:5900-7.
37. Ramalingam SS, Owonikoko TK, Behera M, Subramanian J, Saba NF, Kono SA, et al. Phase II study of docetaxel in combination with everolimus for second- or third-line therapy of advanced non-small-cell lung cancer. J Thorac Oncol. 2013;8:369-72.
38. Besse B, Leighl N, Bennouna J, Papadimitrakopoulou VA, Blais N, Traynor AM, et al. Phase II study of everolimus-erlotinib in previously treated patients with advanced non-small-cell lung cancer. Ann Oncol. 2014;25:409-15.
39. Herrera VA, Zeindl-Eberhart E, Jung A, Huber RM, Bergner A. The dual PI3K/mTOR inhibitor BEZ235 is effective in lung cancer cell lines. Anticancer research. 2011;31:849-54.
40. Fiebig HH, Neumann HA, Henss H, Koch H, Kaiser D, Arnold H. Development of three human small cell lung cancer models in nude mice. Recent Results Cancer Res. 1985;97:77-86.
41. Hidalgo M, Amant F, Biankin AV, Budinska E, Byrne AT, Caldas C, et al. Patient-derived xenograft models: an emerging platform for translational cancer research. Cancer Discov. 2014;4:998-1013.
42. Montero J, Sarosiek KA, DeAngelo JD, Maertens O, Ryan J, Ercan D, et al. Drug-induced death signaling strategy rapidly predicts cancer response to chemotherapy. Cell. 2015;160:977-89.
43. Frese KK, Tuveson DA. Maximizing mouse cancer models. Nat Rev Cancer. 2007;7:645-58.
44. Schuurbiers OC, Kaanders JH, van der Heijden HF, Dekhuijzen RP, Oyen WJ, Bussink J. The PI3-K/AKT-pathway and radiation resistance mechanisms in non-small cell lung cancer. J Thorac Oncol. 2009;4:761-7.

## Figure Legends

**Figure 1**. **CYD-2-11 compound selectively binds to Bax protein and induces apoptosis in various NSCLC and SCLC cell lines**. **A**, Design of CYD-2-11 based on SMBA1. **B**, Synthesis of CYD-2-11. Reactions and conditions: a) salicylaldehyde, KF-$Al_2O_3$, MeOH, 72% yield; b) *tert*-butyl (2-hydroxyethyl)carbamate, DIAD, $PPh_3$, THF, rt, 12 h; c) TFA, $CH_2Cl_2$, rt, 73% yield (2 steps). **C**, Molecular docking of CYD-2-11 into the S184 binding pocket in the C-terminus of Bax protein. **D**, Binding affinities of CYD-2-11 with Bax protein and other Bcl2 family members were analyzed using a competition fluorescence polarization assay. Error bars represent ±S.D. **E**, Levels of pBax and total Bax were analyzed by Western blot in BEAS-2B, NSCLC and SCLC cell lines. **F**, A panel of NSCLC and SCLC cell lines were treated with SMBA1 (5 μM) or CYD-2-11 (5 μM) for 48 hr. Apoptotic cell death was determined by analyzing Annexin-V/PI binding by fluorescence-activated cell sorter (FACS). Error bars represent ± standard deviation (SD) of three separate determinations.

**Figure 2. CYD-2-11 directly induces Bax oligomerization, facilitates Cyt c release and suppresses lung cancer in dose-dependent manner in vivo**. **A**, Bax and BAK expression was analyzed by Western blot following treatment of A549 cells with CYD-2-11 for 24h. **B**, Mitochondria were isolated from A549 cells and then treated with CYD-2-11 or SMBA1 (5 μM) in cross-linking buffer for 30 min at 30 $^{o}$C, followed by cross-linking using BMH. Bax was analyzed by Western blot (B, left panel). A549 cells were treated with CYD-2-11 or SMBA1 (5 μM) for 24h, followed by isolation of mitochondria and cross-linking using BMH. Bax was analyzed by Western blot (B, right panel). **C**, A549 cells were treated with increasing concentrations of CYD-2-11 for 24h. Mitochondrial and cytosolic fractions were isolated. Levels of Cyt *c* and Bax in these two fractions were analyzed by Western blot. Prohibitin were used as

positive control to verify mitochondrial fraction without contamination. **D**, Nu/Nu mice with A549 lung cancer xenografts were treated with increasing doses of CYD-2-11 (2~40 mg/kg/d) i.p. for 10 days. Each group included 8 mice. Tumor volume was measured once every 2 days. The error bars indicate ± SD (n= 8). **E** and **F**, Active caspase 3 was analyzed in tumor tissues at the end of experiments by IHC staining. The error bars indicate ± SD of three separate determinations. **G**, Mitochondria were isolated from tumor tissues, and followed by cross-linking using BMH. Bax was analyzed by Western blot.

**Figure 3. Efficacy of SMBA1 and CYD-2-11 was compared in NSCLC and SCLC xenografts**. **A**, Nu/Nu mice with NSCLC (A549) or SCLC (DMS53) xenografts were treated with 40 mg/kg of SMBA1 or CYD-2-11 i.p. for 14 days. Each group included 8 mice. Tumor volume was measured once every 2 days. The error bars indicate ± SD (n=8). **B**, Active caspase 3 was analyzed in tumor tissues at the end of experiments by IHC staining. The error bars indicate ± SD of three separate determinations. **C**, Mitochondria were isolated from tumor tissues after treatment of mice with SMBA1 or CYD-2-11, and followed by cross-linking using BMH. Bax was analyzed by Western blot.

**Figure 4. CYD-2-11 represses tumor growth in SCLC patient-derived xenografts. A**, Mice carrying xenografts derived from two patients with refractory SCLC (TKO-002 or TKO-005) were treated with CYD-2-11 (40 mg/kg/d) i.p. for 2 weeks. Tumor volumes were analyzed. Error bars represent ± S.D (n=6). **B**, pBax and 6A7 Bax were analyzed in tumor tissues at the end of experiments by QD-IHF as described in “Supplemental Methods”. **C**, Mitochondria were isolated from tumor tissues after treatment of mice with CYD-2-11, and followed by cross-linking using BMH. Bax was analyzed by Western blot. **D**, Active caspase 3 was analyzed by

IHC and quantified in tumor tissues at the end of experiments. The error bars indicate ± SD of three separate determinations.

**Figure 5. CYD-2-11 suppresses lung cancer growth and prolongs survival in genetically engineered mouse models (GEMM). A**, After administration of adenovirus Cre recombinase in $KRAS^{G12D}$ $LKB1^{fl/fl}$ (KL) mice for 6 weeks, KL mice were treated with CYD-2-11 for 8 weeks (control group, 8 mice, treatment group, 7 mice). Tumor numbers were counted under the microscope and tumor area was quantified using Openlab modular imaging software. **B**, Three representative H&E images from control or treatment group were shown. **C**, Active caspase 3 was analyzed by IHC at the end of experiments. **D**, Survival of mice was calculated up to 8 weeks before euthanization in the control group versus CYD-2-11 treatment group.

**Figure 6. Treatment of lung cancer cells or NSCLC patients with RAD001 upregulates Bax phosphorylation. A** and **B**, A549 cells were treated with RAD001 for 24h. pBax, pAKT and p-p70S6K were analyzed by Western blot or QD-IHF. **C** and **D**, 10 patients with NSCLC were treated with RAD001 (10 mg/day) for 28 days. pBax in tumor tissues was analyzed by IHC and quantified by analyzing immunoscore. Error bars represent ± SD of three separate determinations.

**Figure 7. Combination of CYD-2-11 and RAD001 synergistically represses lung cancer and overcomes rapalog resistance *in vivo*.** Nu/Nu mice with A549 or A549-RR lung cancer xenografts were treated with RAD001, CYD-2-11 or the combination i.p. for 14 days. Each group included 6 mice. (**A**)Tumor volumes were analyzed. Error bars represent ± S.D (n=6). (**B-C**) pBax, 6A7 Bax, pAKT, p-p70S6K and active caspase 3 in tumor tissues were analyzed by QD-IHF or IHC. Error bars represent ± SD of three separate determinations.

Author Manuscript Published OnlineFirst on April 5, 2017; DOI: 10.1158/0008-5472.CAN-16-2356
Author manuscripts have been peer reviewed and accepted for publication but have not yet been edited.

Fig. 1

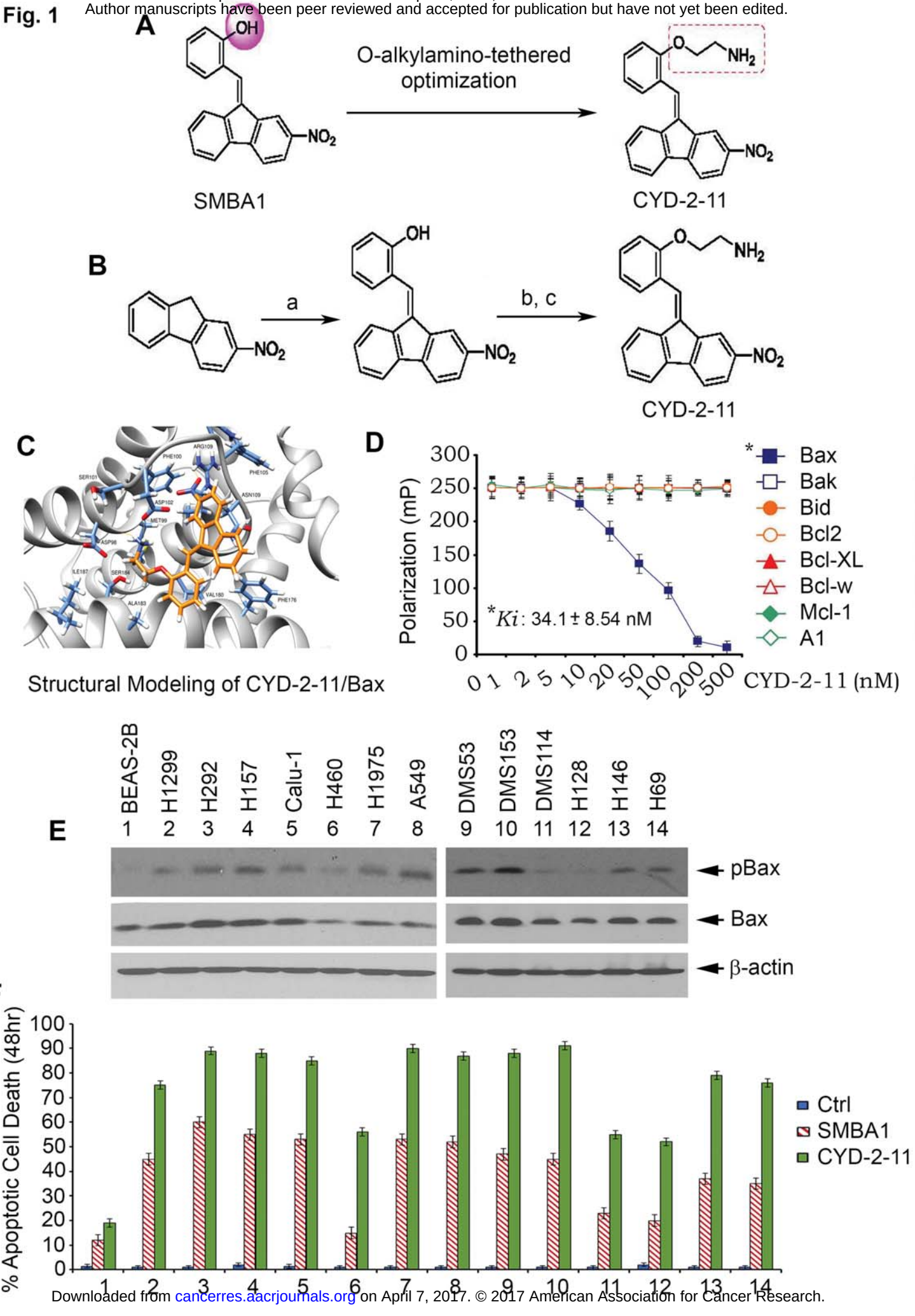

Fig. 2

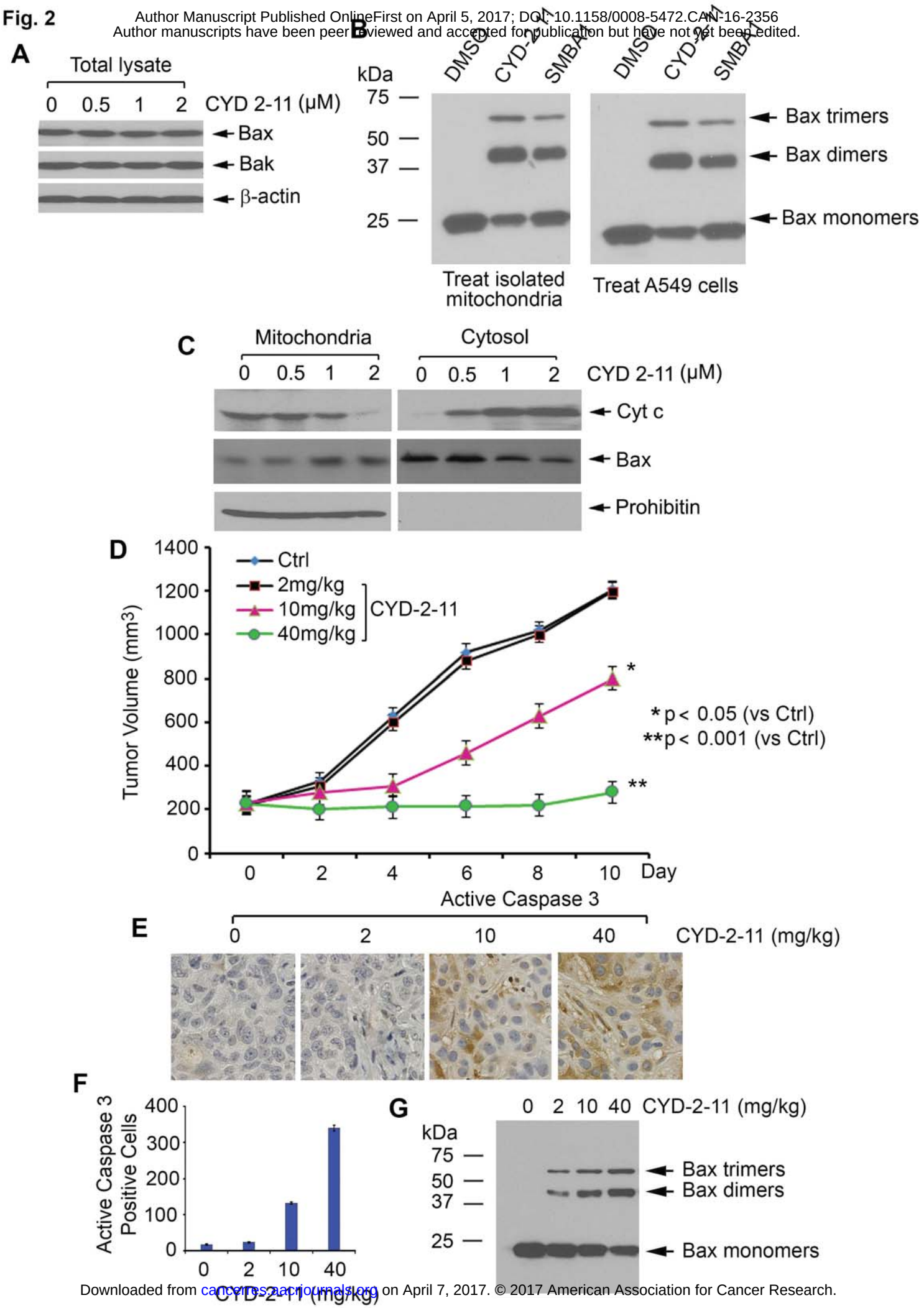

Author Manuscript Published OnlineFirst on April 5, 2017; DOI: 10.1158/0008-5472.CAN-16-2356
Author manuscripts have been peer reviewed and accepted for publication but have not yet been edited.

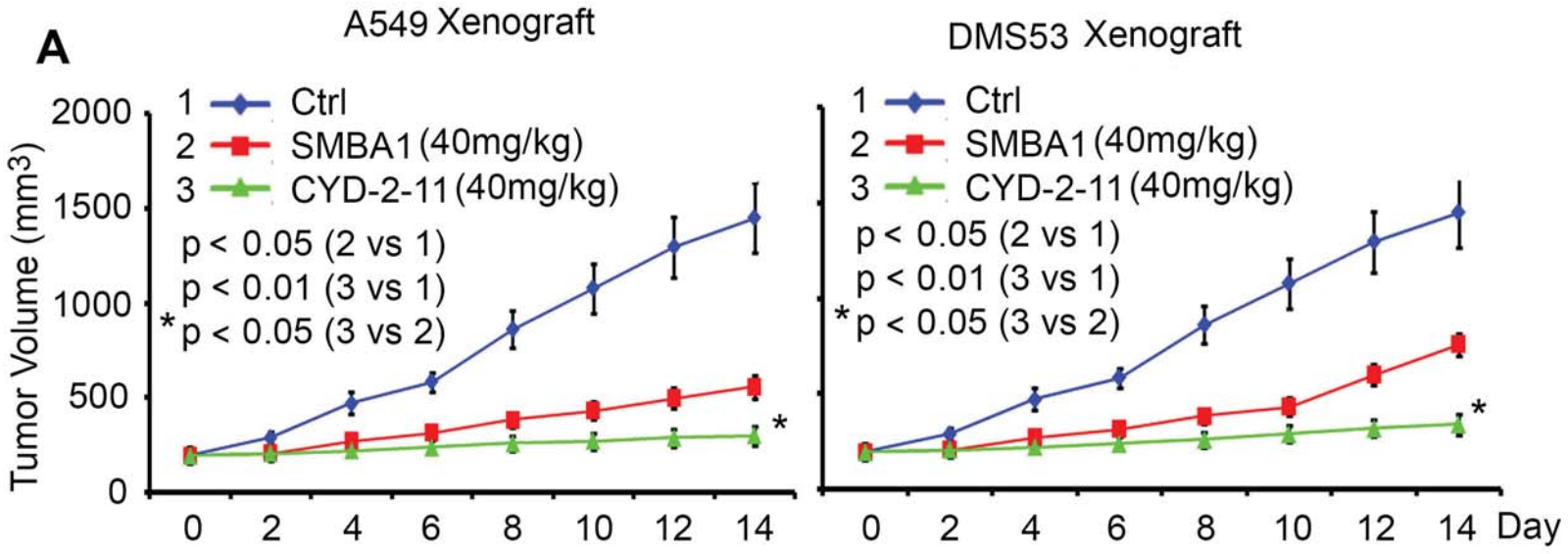


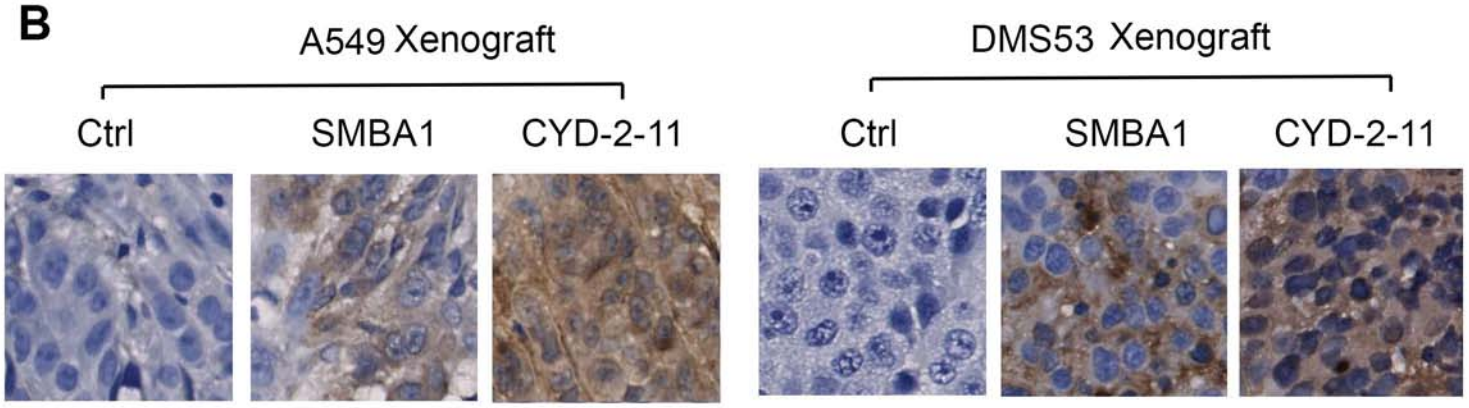


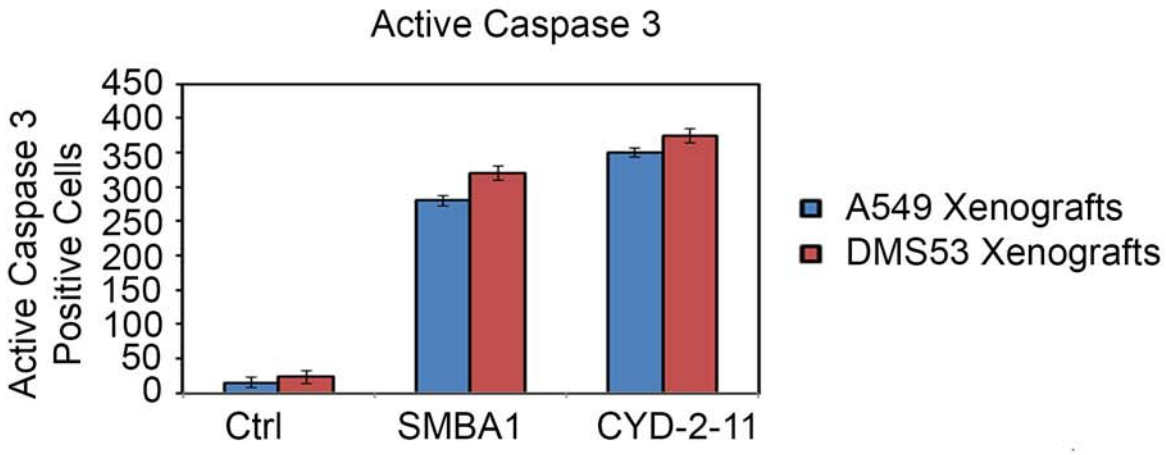


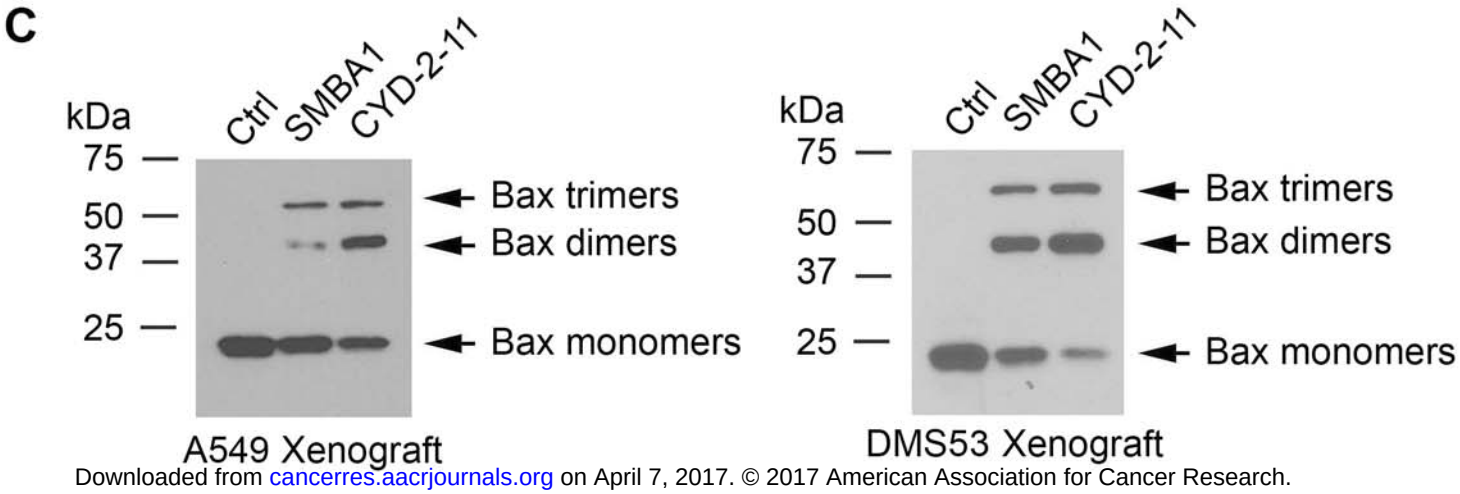

Author Manuscript Published OnlineFirst on April 5, 2017; DOI: 10.1158/0008-5472.CAN-16-2356
Author manuscripts have been peer reviewed and accepted for publication but have not yet been edited.

Fig. 4

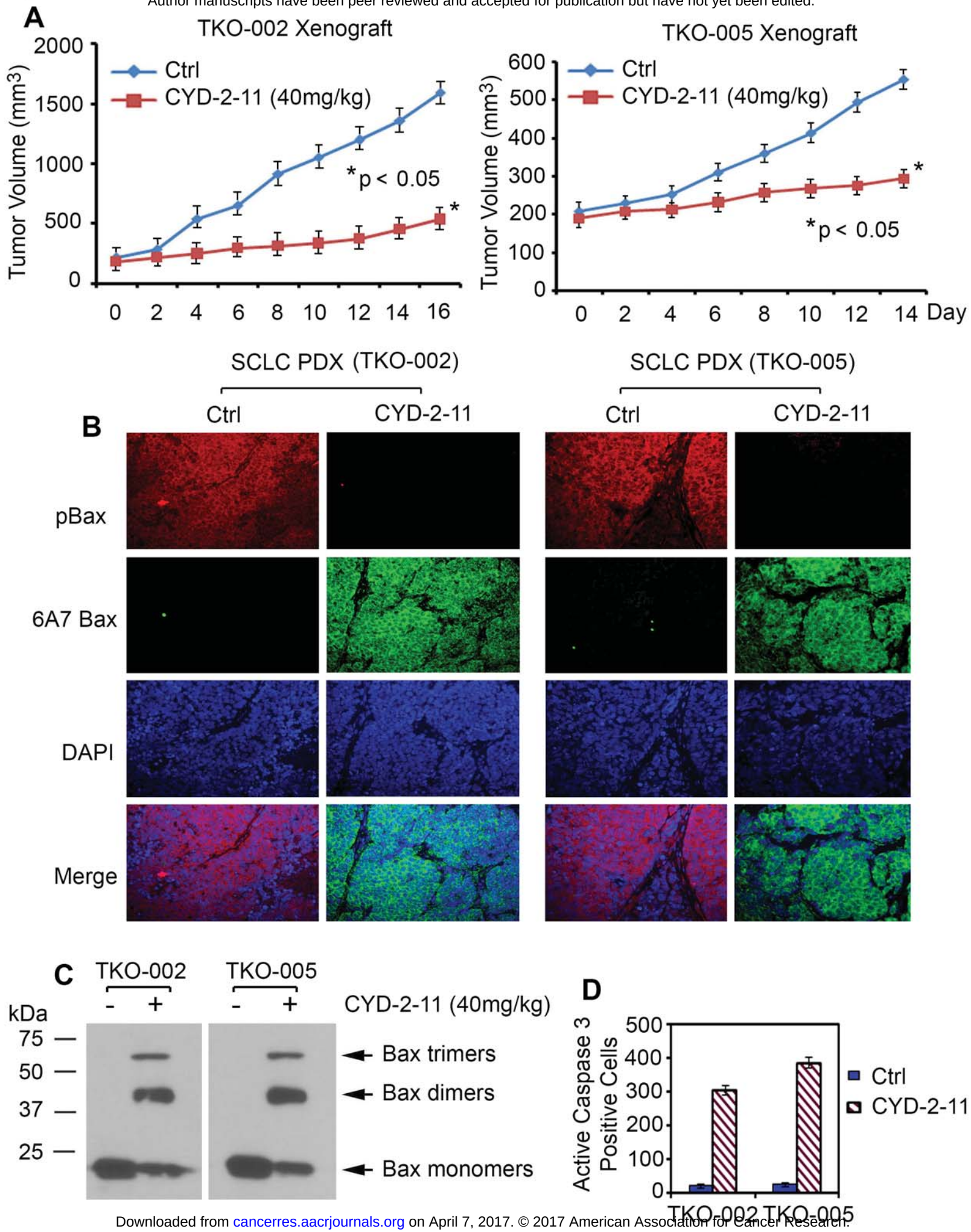

Author Manuscript Published OnlineFirst on April 5, 2017; DOI: 10.1158/0008-5472.CAN-16-2356
Author manuscripts have been peer reviewed and accepted for publication but have not yet been edited.

**Fig. 5**

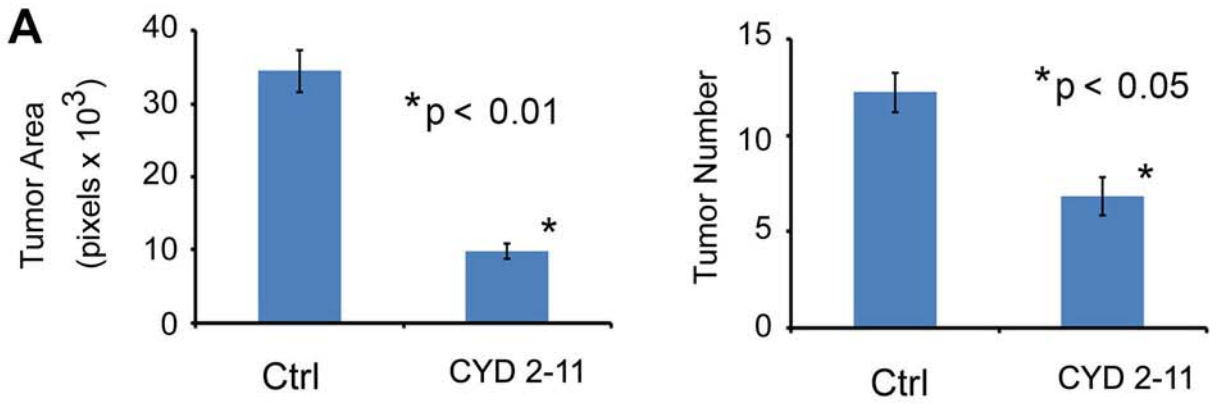


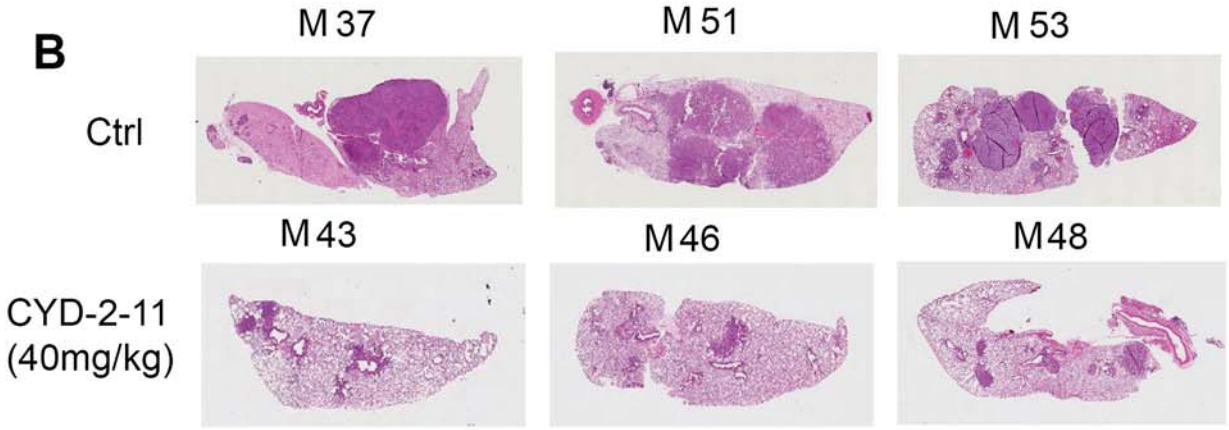


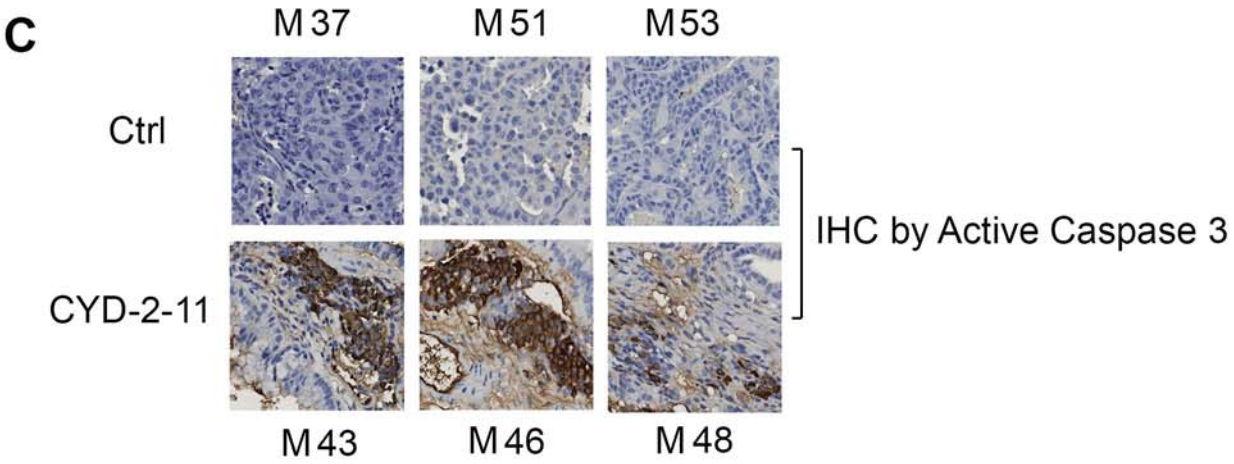


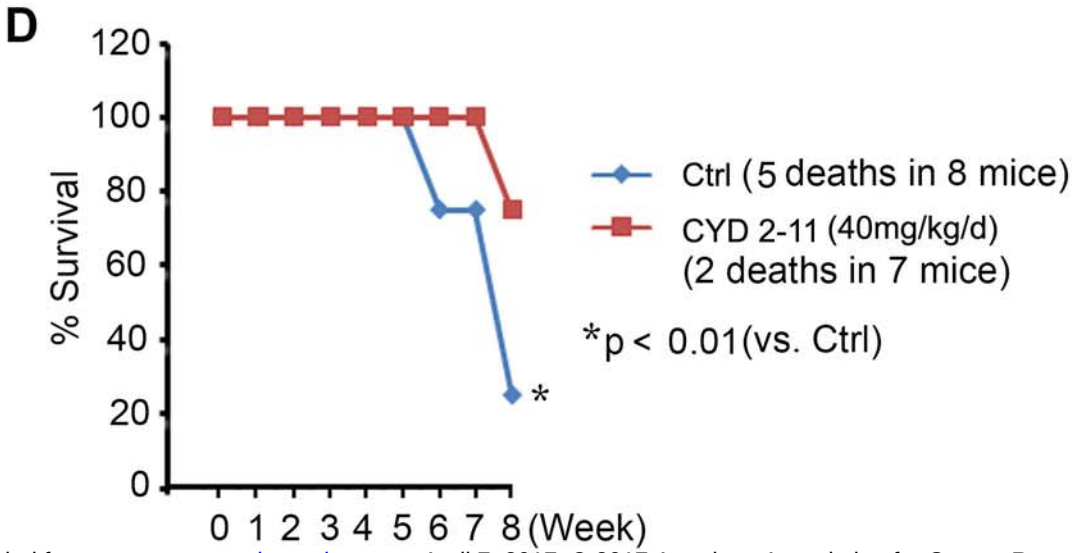

Author Manuscript Published OnlineFirst on April 5, 2017; DOI: 10.1158/0008-5472.CAN-16-2356
Author manuscripts have been peer reviewed and accepted for publication but have not yet been edited.

**Fig. 6**

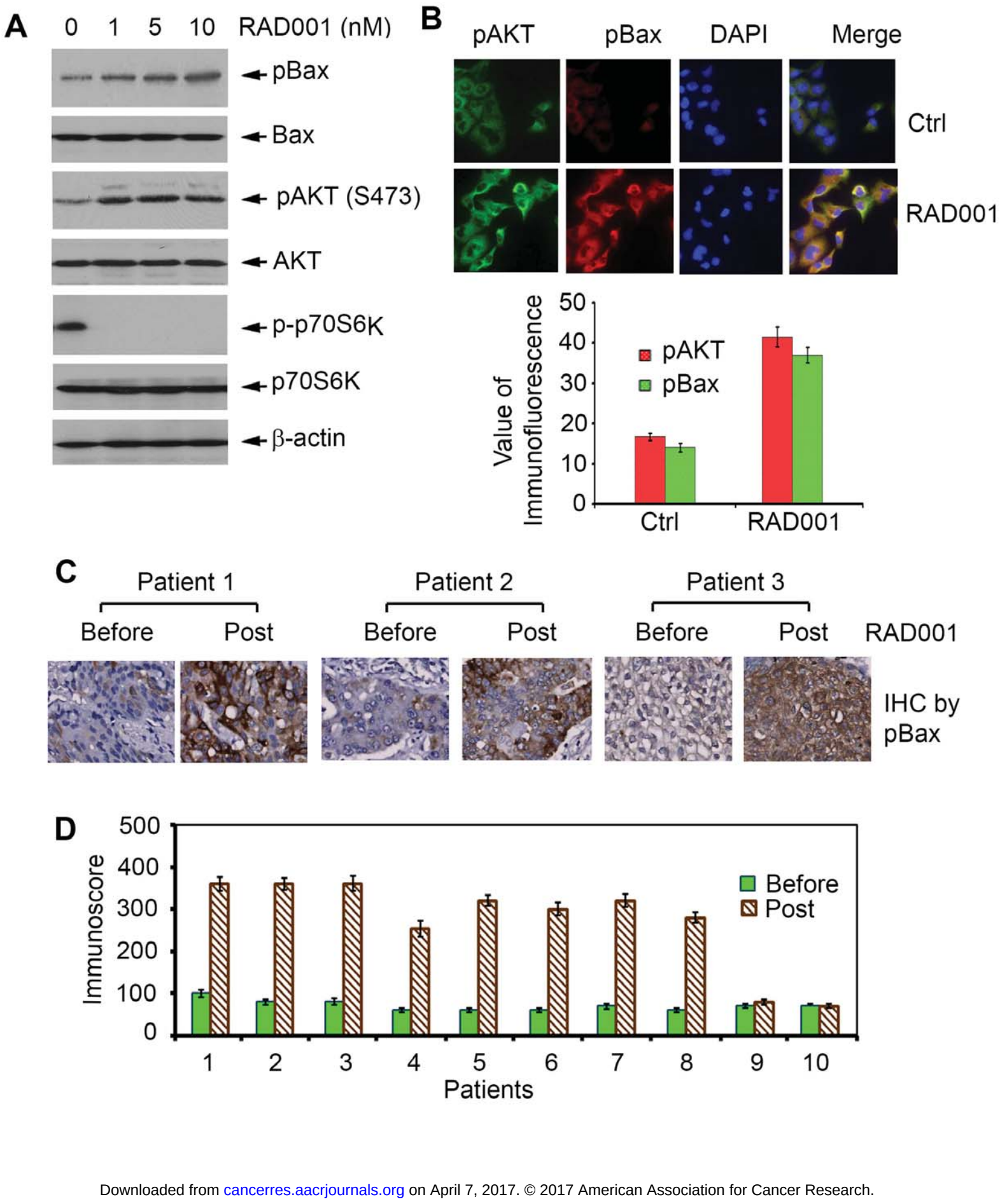

Fig. 7

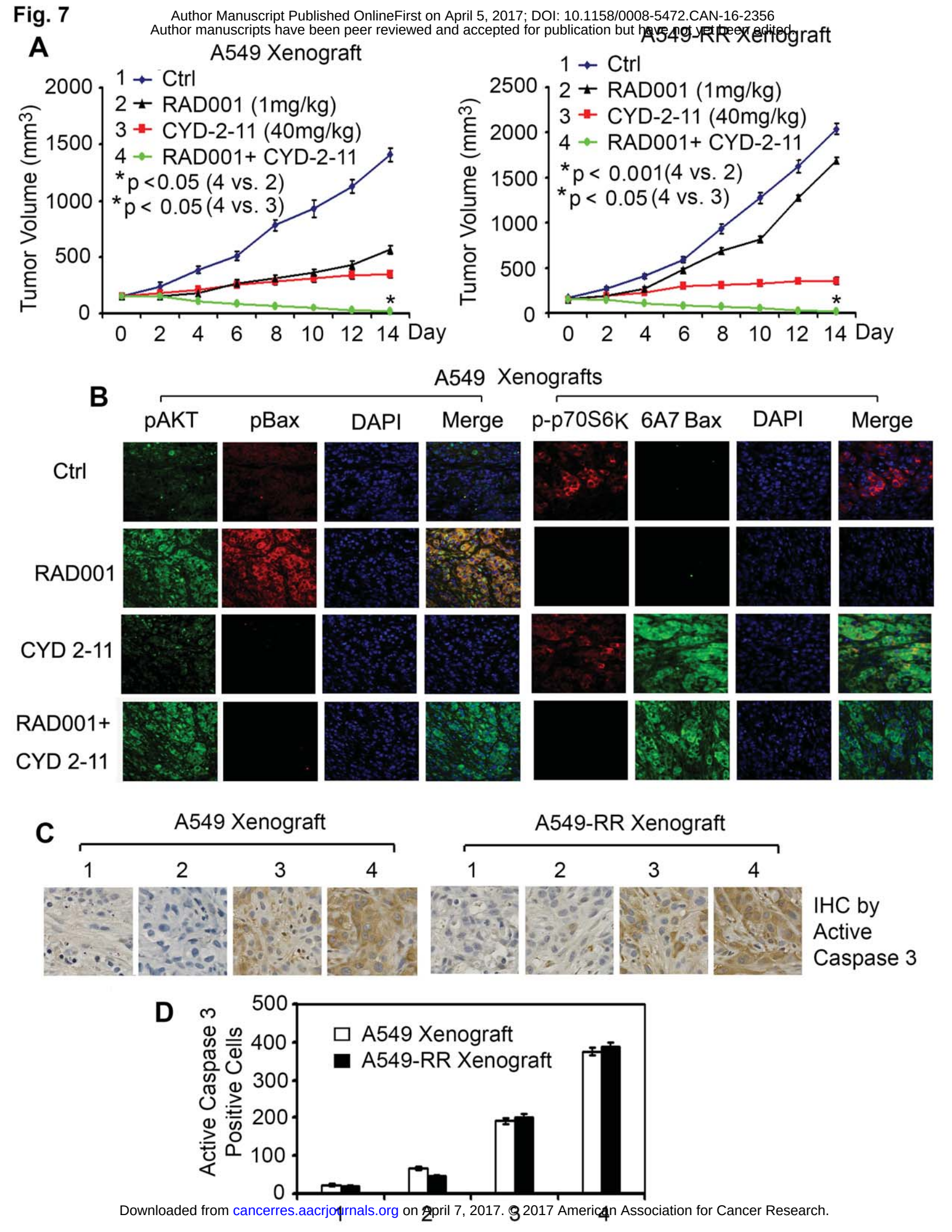

AACR American Association for Cancer Research

Cancer Research

The Journal of Cancer Research (1916–1930) | The American Journal of Cancer (1931–1940)

# Modulation of Bax and mTOR for cancer therapeutics

Rui Li, Chunyong Ding, Jun Zhang, et al.

*Cancer Res* Published OnlineFirst April 5, 2017.